Thallium-201 SPECT and Technetium-99m-Phytate Subtraction Liver Imaging in the Evaluation of Pancreatic Cancers

Kazuyoshi Suga, Kazuya Nishigauchi, Norihiko Kume, Takeshi Fujita, Takashi Nakanishi, Tatsunori Hamasaki and Takashi Suzuki

Departments of Radiology and Second Surgery, Yamaguchi University School of Medicine, Kogushi, Japan

We preliminarily evaluated the usefulness of ^{201}Tl SPECT in the investigation of pancreatic cancers. **Methods:** The subjects included 32 patients with malignant tumors, 16 with benign disorders and 10 controls. SPECT was performed 10 min after the injection of 148–222 MBq of ^{201}Tl; subjects had fasted to minimize intestinal activity. In addition, subtracted SPECT using ^{99m}Tc-phytate to separate the boundary of abnormal uptake from liver activity was carried out in 14 patients. **Results:** Thallium-201 did not accumulate in the pancreatic bed of the controls. In contrast, 29 of the 32 patients with malignant tumors showed positive phytate uptake with a sensitivity of 90.6% in the detection of malignancy. Of the 16 benign disorders, only four patients showed abnormal uptake; however, the mean value of the lesion-to-hepatic ratio (0.43 ± 0.06; range, 0.35–0.51), as an index of the degree of uptake, was lower than that in positive malignant tumors (0.72 ± 0.16; range, 0.53–1.28). Thallium-201 activity per milligram of resected cancer tissue in two patients was 2–3 times greater than in normal tissue. Follow-up ^{201}Tl SPECT in the five treated patients demonstrated similar alterations between ^{201}Tl uptake and tumor markers. **Conclusion:** Our results suggest that ^{201}Tl SPECT may have clinical potential in the investigation of pancreatic cancers.

Key Words: thallium-201-chloride; pancreatic cancer; chronic pancreatitis; single-photon emission computed tomography; technetium-99m-phytate

J Nucl Med 1995; 36:762–770

The diagnostic work-up of patients with pancreatic cancer remains a difficult clinical challenge, even with the use of many imaging techniques. A radionuclide study is infrequently used in pancreatic cancers because of the absence of suitable radiopharmaceuticals that can depict them positively. Selenium-75-selenomethionine and [^{125}I]-N,N,N′-trimethyl-N′-(2-hydroxy-3-methyl-5-iodobenzyl)-1,3-propanediamine (^{123}I-HIPDM) accumulate in normal pancreatic tissue, but neither agent can positively depict tumors (*1–3*) and are not currently utilized. The high affinity of ^{18}F-deoxyglucose for pancreatic cancers has been demonstrated (*4*). Unfortunately, PET is not a routine procedure due to its complexity and limited availability.

There are numerous reports of ^{201}Tl-chloride avidity in various malignant tumors, especially in adenocarcinomas (*5–8*). Rotational SPECT has improved the ability to depict radiopharmaceutical distribution from structures deep within the body. Thus, it is expected that ^{201}Tl accumulates in pancreatic tumors and that ^{201}Tl SPECT can sensitively detect it, even in the deeply located pancreatic beds.

Thallium-201 accumulates in malignant tumors mainly by sodium-potassium adenosine triphosphatase activity in cell membranes (*9–14*), and its uptake is considered to be related to the viability and proliferative potential of tumor cells (*12–16*). Recent studies have shown that a change in ^{201}Tl in treated tumors indicates therapeutic response (*17–21*). Therefore, this agent may play a role in monitoring treatment response in pancreatic cancers when such assessment is difficult with other imaging modalities.

METHODS

Subjects

Fifty-eight subjects were investigated from July 1991 to May 1994 at our institution, and all participants gave informed consent. Malignant tumors were found in 30 patients with pancreatic cancer, 1 with choleductal cancer of tubular adenocarcinoma and 1 with primary malignant lymphoma (18 men and 14 women, ages 43–87 yr) (Table 1). Of the 30 patients with pancreatic cancer, the diagnosis in 27 was surgically proven. Nine of the 27 patients were diagnosed as having adenocarcinomas that were still indeterminate as papillary or tubular type. The remaining three tumors were not proven histologically, but were diagnosed by clinical course, markedly elevated serum levels of CA 19-9 and typical malignant appearance on x-ray computed tomography (CT), magnetic resonance (MR) imaging, ultrasonography (US), endoscopic retrograde-pancreatography (ERP) and angiography.

To investigate benign disorders, four patients with surgically proven benign tumors, one with a congenital simple cyst, ten patients with clinically diagnosed chronic pancreatitis and one with acute pancreatitis were studied (Table 2). The 10 patients with chronic pancreatitis underwent ERP, and mild or severely beaded, dilated appearances of the mean pancreatic duct were

Received Jul. 18, 1994; revision accepted Nov. 23, 1994.
For correspondence or reprints contact: Kazuyoshi Suga, Department of Radiology, Yamaguchi University School of Medicine, Kogushi 1144, Ube, Japan 755.

TABLE 1
Thallium-201 Results for Malignant Tumors

Patient no.	Sex	Age	Site	Size (mm)	Histology	^{201}Tl uptake		Lesion-to-liver ratio	CA 19-9 (U/ml)	Attenuation corrected L/H lesion ratio
						Planar	SPECT			
1	F	78	Head	30	Tubul adenoca.	−	+	0.83	870.0	0.92
2	M	54	Uncus	30	Papil adenoca.	−	+	0.62	*	0.64
3	M	64	Uncus	45	Tubul adenoca.	−	+	0.85	347.0	0.92
4	F	52	Head	30	Papil adenoca.	−	+	0.65	3355.0	0.68
5	F	43	Body	75	Unknown	−	+	0.62	1520.0	0.75
6	M	61	Body	50	Papil adenoca.	−	+	0.59	214.7	0.70
7	F	71	Head	95	Papil adenoca.	+	+	1.28	*	1.44
8	F	60	Head	30	Papil adenoca.	−	+	0.84	37.3	0.94
9	F	52	Head	30	Papil adenoca.	−	+	0.78	80.1	0.85
10	M	70	Head	50	Papil adenoca.	+	+	0.96	41.1	1.08
11	M	63	Head	55	Papil adenoca.	−	+	0.61	10067.0	0.73
12	F	59	Head	60	Adenoca.	+	+	0.81	54318.1	0.91
13	M	87	Head	28	Tubul adenoca.	−	+	0.59	95.0	0.70
14	F	61	Head	25	Tubul adenoca.	−	+	0.73	1817.2	0.79
15	M	79	Head	35	Adenoca.	−	+	0.81	608.3	0.92
16	M	67	Head	34	Papil adenoca.	−	+	0.58	373.1	0.69
17	M	58	Head	40	Papil adenoca.	−	+	0.75	109.4	0.78
18	M	78	Uncus	45	Adenoca.	−	+	0.55	52.8	0.66
19	M	71	Head	30	Papil adenoca.	+	+	0.92	*	1.03
20	F	78	Head	30	Papil adenoca.	−	+	0.59	818.4	0.70
21	F	69	Uncus	32	Adenoca.	−	+	0.87	163.7	0.98
22	M	63	Head	60	Unknown	−	+	0.65	11260.2	0.73
23	M	68	Head	30	Adenoca.	−	+	0.66	20.7	0.69
24	F	63	Uncus	35	Unknown	−	+	1.01	40073.1	1.21
25	M	52	Head	53	Adenoca.	−	+	0.55	17800.0	0.67
26	M	62	Head	30	Mucinous cystadenoca.	−	+	0.57	41.9	0.69
27	F	69	Uncus	28	Adenoca.	−	+	0.53	561.8	0.65
28	M	63	Head	25	Choleductal tubul adenoca.	−	+	0.66	54.0	0.75
29	F	48	Head	40	Malignant lymphoma	−	+	0.64	12.4	0.72
30	M	43	Head	18	Adenoca.	−	−	—	10.0	—
31	M	79	Head	28	Adenoca.	−	−	—	*	—
32	F	76	Tail	30	Tubul adenoca.	−	−	—	1182.9	—

*Normal value of serum CA 19-9 level: <37 U/ml. Patients No. 2, 7, 19, 28 and 31 had Lewis blood type negative, which resulted in a lack of elevated serum CA 19-9 levels.

Tubul adenoca. = tubular adenocarcinoma and Papil adenoca. = papillary adenocarcinoma.

demonstrated, with or without calcification. One patient had a pseudocyst concomitantly, and two formed a focal mass with calcification.

Furthermore, 10 patients, who had undergone ^{201}Tl SPECT for lung cancer and whose lung tumors were located in the lower lung field adjacent to the diaphragm (7 men and 3 women, ages 54–78 yr), were used as controls. The upper abdomen was depicted concomitantly on the SPECT image so that the presence or absence of ^{201}Tl uptake in the pancreatic bed could be evaluated (Fig. 1). For these patients, the pancreas appeared normal on US and CT, and serum amylase levels were within normal limits.

Tumor or lesion size was measured at the longest axis of the tumor on the US, CT or MR images. In the initial phase of dynamic contrast-enhancement CT and MR studies, 28 of the 32 malignant tumors showed lower attenuation or intensity than normal parenchyma, indicating hypoperfusion; although two of the three benign tumors (serous cystadenoma and insulinoma) were markedly enhanced. Secondary dilatation of the pancreatic duct in the caudal pancreatic parenchyma was noted in 19 of the 32 malignant tumors.

Thallium-201 SPECT

Each patient fasted prior to ^{201}Tl scintigraphy for more than 12 hr to suppress ^{201}Tl uptake in the small intestine (*7,22,23*), whereas 14 patients did not need this preparation since they had already fasted and had received hyperalimentation intravenously.

Thallium-201 was intravenously injected at a dose of 148–222 MBq, which is higher than usual doses used for myocardial perfusion imaging, to obtain better counting statistics and image quality. Five minutes later, the planar image was initially taken by a rotating gamma camera system fitted with a low-energy, high-resolution collimator with a single-head detector using a one-peak energy window centered over 80 keV with a width of 20%. A preset count of 1,000,000 was used for anterior and posterior views.

TABLE 2
Thallium-201 Results for Benign Disorders

Patient	Sex	Age	Site	Size (mm)	Histology	^{201}Tl uptake		Lesion-to-liver ratio	CA 19-9 (U/ml)	Attenuation corrected L/H ratio
						Planar	SPECT			
1	M	73	Tail	55	Insulinoma	–	+	0.35	908.6	0.39
2	F	73	Uncus	90	Serous cystadenoma	–	+	0.51	46.2	0.58
3	M	44	Diffusely swollen		Acute pancreatitis	–	+	0.48	—	0.54
4	M	44	Head ~ Body (calcified)	40	Focal chr. pancreatitis	–	+	0.41	44.1	0.48
5	M	70	Tail	32	Mucinous cystadenoma	–	–	—	*	—
6	F	71	Uncus	20	Papil adenoma	–	–	—	0.4	—
7	F	75	Body	50	Simple cyst	–	–	—	—	—
8	M	53	Head	25	Pseudocyst with chr. pancreatitis	–	–	—	145.2	—
9	M	48	Diffusely (calcified)		Chr. pancreatitis	–	–	—	56.3	—
10	M	68	Head ~ Uncus (calcified)	35	Focal chr. pancreatitis	–	–	—	32.4	—
11	M	56	Diffusely		Chr. pancreatitis	–	–	—	31.8	—
12	M	75	Diffusely (calcified)		Chr. pancreatitis	–	–	—	22.5	—
13	M	61	Diffusely		Chr. pancreatitis	–	–	—	37.1	—
14	M	57	Diffusely		Chr. pancreatitis	–	–	—	24.6	—
15	M	64	Diffusely		Chr. pancreatitis	–	–	—	—	—
16	F	42	Diffusely		Chr. pancreatitis	–	–	—	41.5	—

*Normal value of serum CA 19-9 levels <37 U/ml.
Chr. pancreatitis = chronic pancreatitis. Patient 5 had Lewis blood type negative.

Subsequently, the SPECT image was acquired using 360° rotation at 60 intervals in a 64 × 64 matrix. The acquisition time of each projection was 30 sec. Projection data were preprocessed with a Butterworth filter (order, 8; cutoff frequency 0.25) and the transaxial and coronal images were reconstructed by ramp filter backprojection; the slice thickness was 6.4 mm. The FWHm of the system was 12.5 mm at the center of rotation with a rotation radius of 20 cm; attenuation correction was not performed.

When the boundary between abnormal ^{201}Tl uptake and adjacent liver activity was unclear on the first ^{201}Tl SPECT image, 111 MBq of ^{99m}Tc-phytate were injected and a subsequent SPECT image was acquired for differentiation 20 min later. Patients remained on the imaging table throughout both imaging sessions and were instructed not to move during and between sessions to minimize artifacts. Phytate SPECT images were acquired using the same collimator as the initial ^{201}Tl SPECT image, with a one-peak energy window of 140 keV ±15% (*24*). Acquisition conditions were the same for both scans. The transaxial liver image was reconstructed in the same manner as the ^{201}Tl SPECT image.

The ^{201}Tl and phytate images were compared slice-by-slice onscreen. A 5 × 5 pixel region of interest (ROI) was drawn over the liver areas on the phytate image, avoiding areas of large vessels, and the same sized ROI was superimposed in registry on the corresponding ^{201}Tl image. The constant for subtraction, which is multiplied by the phytate images, was decided by the ^{201}Tl/^{99m}Tc-phytate ratio in the liver, and the phytate images were subtracted from ^{201}Tl images in all slices. Subtraction imaging was performed in the 11 patients with malignant tumors and the three with benign disorders. In these patients, it generally took about 100 min to complete these procedures.

In addition to visual assessment for semiquantitative estimation of the degree of lesional ^{201}Tl uptake, lesion-to-hepatic (L/H) ratios of ^{201}Tl activity were measured from the average counts per pixel obtained by ROIs manually drawn in the abnormal radioactivity in the pancreatic bed and in the ventral portion of the right hepatic lobe (S_8) on the axial sections. Because attenuation correction was not performed, we used those ratios as an index to show the degree of lesional ^{201}Tl uptake.

In tumors with centrally reduced radioactivity, the ROIs were drawn along the contour of abnormal radioactivity, including both the peripheral intense uptake site and the centrally reduced uptake site, because it was difficult to objectively choose the most intense uptake site. The ROIs were placed three times each by three observers, and the mean value of the L/H ratios was calculated.

Attenuation Correction

Attenuation correction in ^{201}Tl SPECT, despite low-energy gamma rays, may be a valid way to ensure more accurate quantitation and to improve image quality (*25,26*). We attempted attenuation correction for all 48 patients with the postcorrection method proposed by Chang (*27*), which uses the GMS 5500-A data processor (Toshiba, Tokyo, Japan). In this procedure, a constant value for effective attenuation coefficient (μ) and an

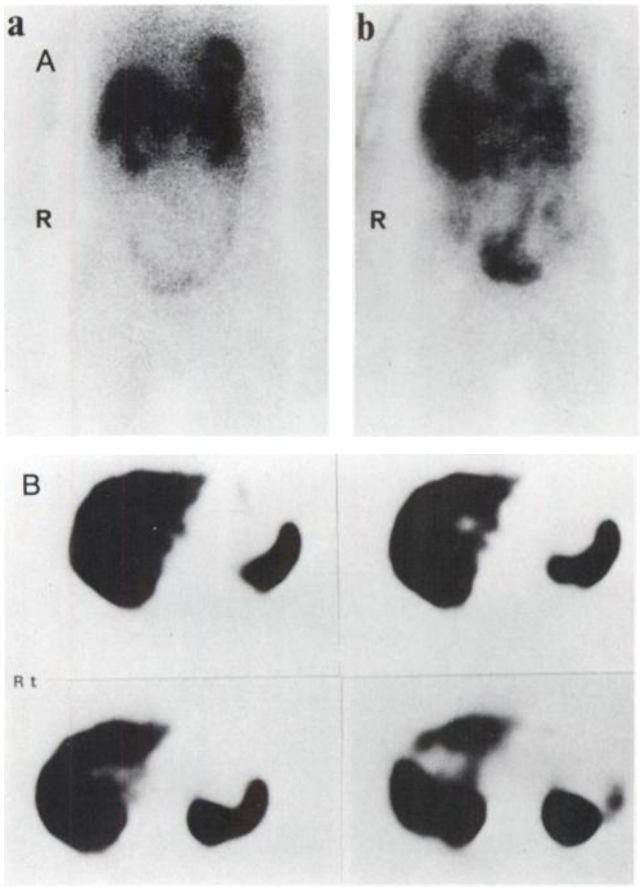

FIGURE 1. Thallium-201 planar (A-a) and SPECT (B) images of a control subject (a 57-yr-old man) after fasting. The planar image demonstrates diminished ^{201}Tl activity in the small intestine compared to the nonfasted control (A-b, a 53-yr-old male). SPECT did not show any abnormal ^{201}Tl uptake in the pancreatic bed.

elliptical contour over the abdomen in each patient was used. The μ value was determined in a body phantom (elliptical torso, major axis dimensions: 28.5 cm, minor axis: 20 cm, length, 30 cm) filled with a uniform concentration of approximately 10 kBq/ml of ^{201}Tl to mimic the patient's abdomen and resulted in $\mu = 0.11$ cm^{-1}. The values of L/H ratios on the corrected images, which were measured using the same ROIs as on the uncorrected images, were compared to the uncorrected values.

Image Interpretation

For prospective evaluation of ^{201}Tl SPECT images, three nuclear medicine specialists experienced in ^{201}Tl scintigraphy (KS, KN and NK) and blinded to the diagnoses and results from other imaging modalities interpreted all images for the presence or absence of abnormal ^{201}Tl uptake in the pancreatic bed and for location of ROI placement. Any disagreement was resolved by consensus. Any focal or diffuse increased uptake in the pancreatic bed was considered abnormal. These findings were then compared with CT and/or MR findings.

Thallium-201 Activity in Resected Specimens

Thallium-201 activity in the resected specimens was investigated in the two patients with pancreatic cancer (Patients 9 and 17). These patients underwent partial tumor resection and total duodenopancreatectomy. Thallium-201 (148 MBq) was injected intravenously 2 hr before resection, and three sample pieces (5.3–191.5 mg) obtained from solid viable tumor tissue, necrotic tumor tissue and surrounding normal pancreatic tissue were weighed immediately. The radioactivities were counted for 10 min in a well-type scintillation counter.

Follow-up Thallium-201 SPECT

Five patients with pancreatic cancer who had positive ^{201}Tl uptake were treated with irradiation and/or hyperthermia. Thallium-201 SPECT was performed to investigate tumoral ^{201}Tl uptake change after this conservative treatment. Imaging occurred 22–45 days after treatment, and the change in L/H ratios was compared with concomitantly measured serum levels of tumor markers (Table 3).

RESULTS

On ^{201}Tl SPECT, physiological ^{201}Tl uptake was always noted most intensely in the kidneys and less intensely in the stomach, liver and spleen. Varying degrees of ^{201}Tl uptake in the small intestine, which formed a continuous loop both on axial and coronal images, were seen; although patients with positive malignant tumors had the most intense uptake. The location of the pancreatic bed could be identified by these positive landmarks and the defective contours of the gallbladder, vertebrae and abdominal great vessels such as aorta and vena cava inferior (Figs. 1–6). Subtracted SPECT imaging allowed us to clarify bound-

TABLE 3
Follow-up Results After Treatment

Patient no.	Treatment	Tumor size (mm)		Tumor-to-liver ratio		CA 19-9 (U/ml)	
		Pre.	Post.	Pre.	Post.	Pre.	Post.
3	IORT	45 × 40	70 × 40	0.85	1.04	347	1032
4	IORT, IOHT	30 × 30	30 × 30	0.65	0.39	3355	564
5	RT, HT	75 × 52	44 × 40	0.62	0.47	1520	821
11	IORT	55 × 50	57 × 54	0.61	0.88	10067	26123
23*	IORT, IOHT	30 × 28	34 × 30	0.66	0.57	(390) (CA-125)	(77)

*Serum CA 125 levels were used to monitor the effect of treatment because CA 19-9 levels before treatment were low (20.7 U/ml).
IORT = intraoperative radiation therapy (20 Gy); IOHT = intraoperative hyperthermia therapy; RT = radiation therapy (40 Gy); HT = hyperthermia therapy (42–43°C for 30–40 min).

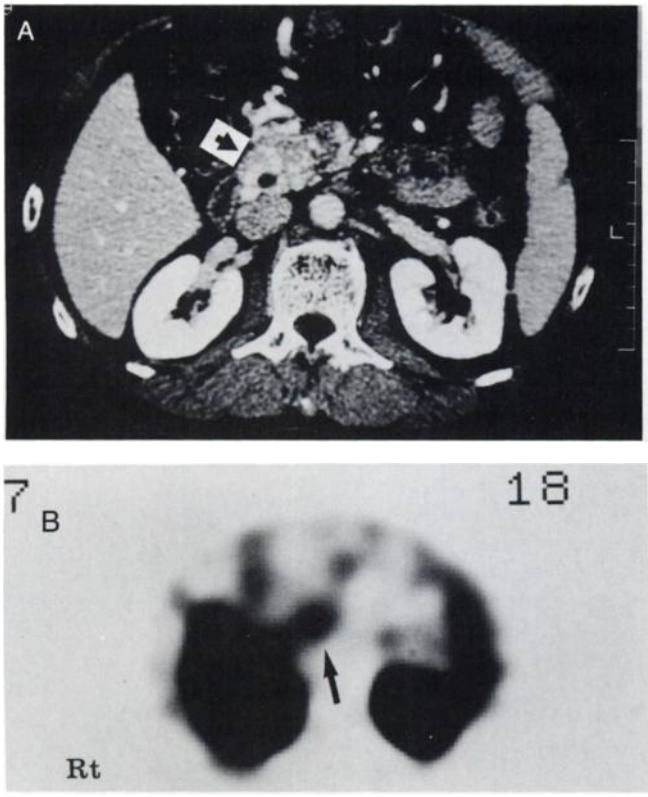

FIGURE 2. A 78-yr-old woman with a tubular adenocarcinoma. (A) Enhanced CT shows a low attenuated 30 × 30-mm tumor in the pancreas head (➡). (B) Thallium-201 SPECT image shows intense uptake corresponding to the tumor, with an L/H ratio of 0.83 (➡).

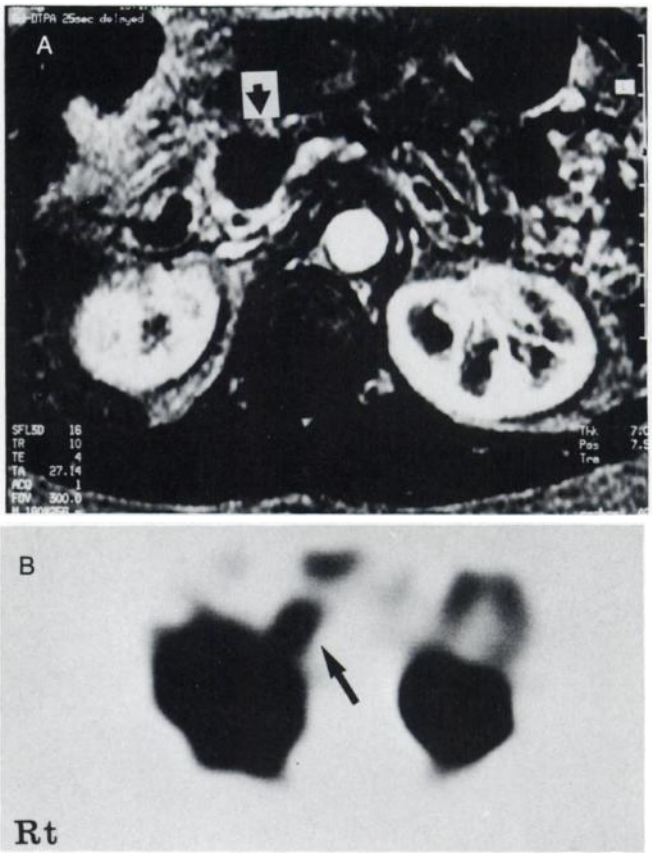

FIGURE 3. A 61-yr-old woman with a tubular adenocarcinoma, which was one of the smallest cancers positively depicted in our series. (A) Dynamic contrast-enhanced, three-dimensional, fast, low-angle image obtained 25 sec p.i. (10/4/1; TR/TE/excitation, flip angle; 16°) shows a hypointense 25 × 20-mm tumor in the pancreas head (➡). (B) Thallium-201 SPECT image shows intense uptake corresponding to the tumor, with an L/H ratio of 0.73 (➡).

aries of abnormal uptake from physiological liver activity (Figs. 4, 5).

Abnormal ^{201}Tl uptake sites corresponded to the lesions seen on CT and/or MR images in all patients. The coefficient of variation of the values of the L/H ratios measured by three observers was 5.2%.

Malignant Tumors

Although the 10 controls did not show ^{201}Tl uptake in the pancreatic bed (Fig. 1), abnormal uptake was seen in 29 (sensitivity, 90.6%) of the 32 patients with a malignant tumor on ^{201}Tl SPECT. In contrast, planar images showed that only four (13.7%) of those tumors were positive. The L/H ratios in the 29 SPECT-positive malignant tumors ranged from 0.53 to 1.28, and the mean value was 0.72 ± 0.16. The two smallest positive malignant tumors were 25 mm in diameter (Patients 14 and 28). In the 19 malignant tumors with secondary dilatation of the caudal pancreatic duct, no obvious abnormal uptake was seen in caudal parenchyma, with or without atrophy. The three negative tumors ranged in size from 18 to 30 mm (Patients 27–29). There seemed to be no clear correlation between L/H ratio and tumor size, histological type or serum CA 19-9 levels.

Benign Disorders

Twelve of the 16 patients with benign disorders had negative ^{201}Tl images, resulting in a specificity of 76.9% for malignancy detection. Although two benign neoplasms, one acute pancreatitis and one focal chronic pancreatitis showed positive ^{201}Tl uptake, the L/H ratios ranged from 0.35 to 0.51 and were lower than the L/H ratios in positive malignant tumors. One patient with acute pancreatitis showed diffuse but faint uptake throughout the entire pancreas. No abnormal ^{201}Tl uptake was noted in the 10 patients with chronic pancreatitis, except for one patient with focal chronic pancreatitis.

Attenuation Correction

Attenuation correction resulted in ^{201}Tl SPECT images with increased lesional count densities and reduced hot rim artifacts seen at the edge of the liver (*25*). Attenuation correction did not, however, affect the sensitivity for detecting abnormal ^{201}Tl uptake nor its distribution within the lesions. The corrected L/H values increased in all patients and differed 3.2%–22.6% (mean ± s.d., 13.6% ± 5.4%) from uncorrected values (Tables 1, 2).

Thallium-201 Activity in Resected Specimens

For Patient 9, the radioactivity (cts/mg/min) in solid viable tumor tissue was 498 ± 57, in necrotic tumor tissue

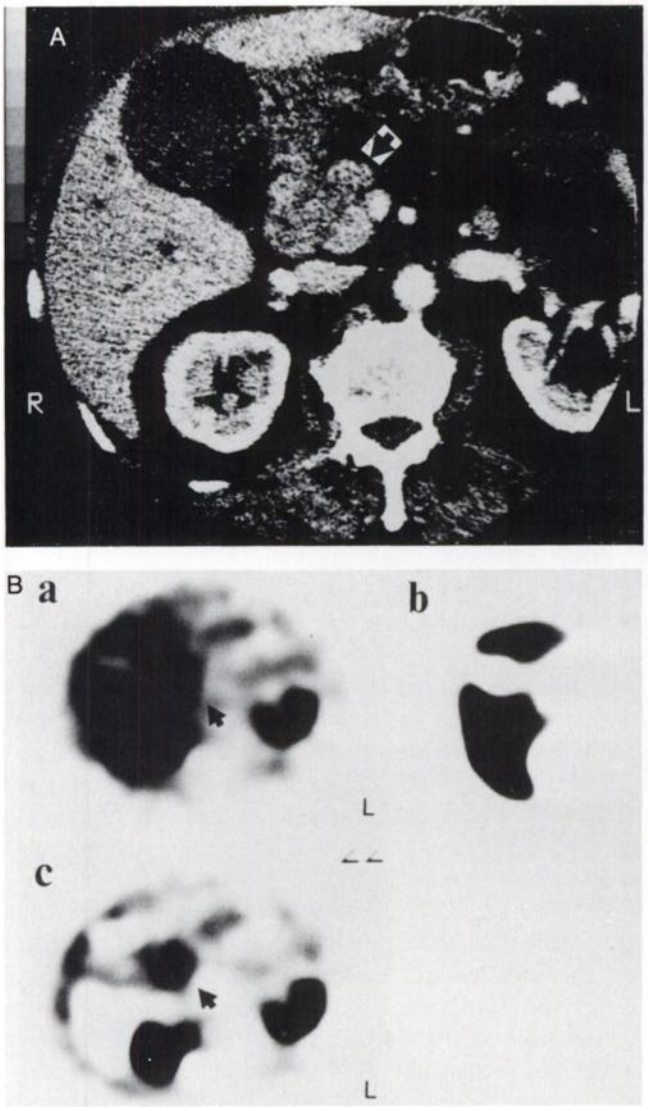

FIGURE 4. A 79-yr-old male with an adenocarcinoma. (A) Enhanced CT shows a 35 × 30 mm tumor in the pancreas head (➡). Secondary dilatation of the pancreatic duct is seen in the caudal portion. (B) On the ^{201}Tl SPECT image (a), the boundary of ^{201}Tl uptake in the tumor (➡) was not clearly distinguished from liver activity. In contrast, the subtracted SPECT image (c), which was obtained using the ^{99m}Tc-phytate image (b), subtracts the liver and an abnormal uptake site was clearly visualized (➡). The L/H ratio acquired on the ^{201}Tl SPECT image (a) was 0.81. Incidentally, no clear abnormal uptake was noted in the caudal portion of the pancreas.

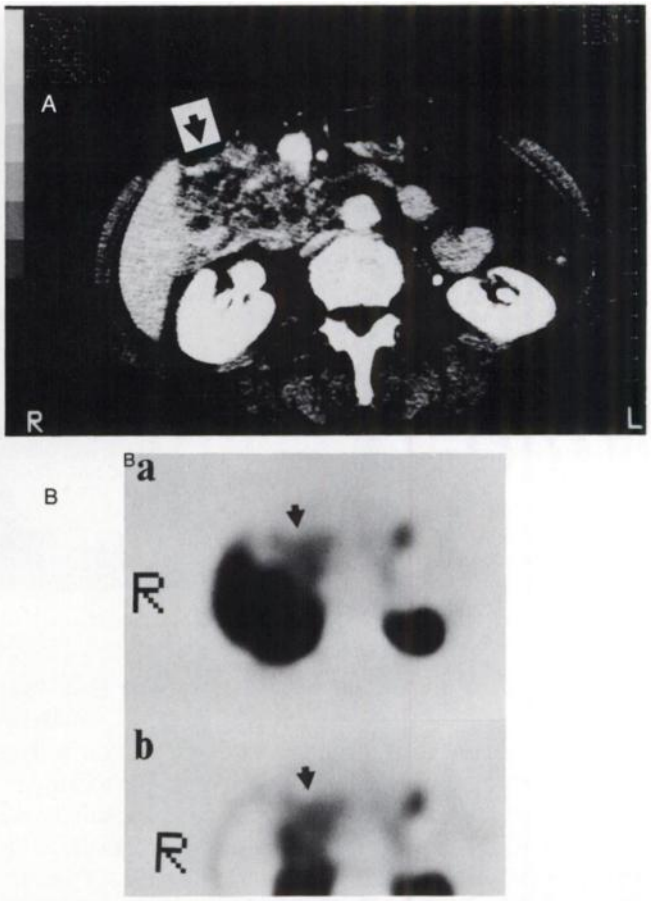

FIGURE 5. A 73-yr-old female with a serous cystadenoma. (A) Enhanced CT shows a large, markedly enhanced mass composed of numerous cystic lesions (➡), measuring 90 × 55 mm in the pancreatic uncus. (B) Tumor uptake of ^{201}Tl (➡) was not clearly distinguished from liver activity on ^{201}Tl SPECT (a). The subtracted SPECT image (b) subtracted the liver and an abnormal uptake site was clearly visualized (➡). The L/H ratio acquired on the ^{201}Tl SPECT image (a) was relatively 0.51.

357 ± 13 and in normal parenchyma 189 ± 34. For Patient 17, the values for these tissues were 191 ± 34, 85 ± 32 and 59 ± 21, respectively. In both patients, ^{201}Tl activity in the solid viable portion of the tumors was two- or three-fold greater than the normal parenchyma.

Follow-up Thallium-201 SPECT

Table 3 shows the follow-up results for five patients with cancer. All patients had a residual or growing tumor on CT after treatment, but showed a similar alteration in L/H ratios as the serum level of the tumor markers. Particularly, three patients (nos. 4, 11, 23) had a similar sized tumor as in pretreatment; however, two of these patients showed diminished tumoral ^{201}Tl uptake with decreased tumor marker levels (Fig. 6); the remaining patient showed increased ^{201}Tl uptake with increased tumor markers.

DISCUSSION

Thallium-201 SPECT had a sensitivity of 90.6% in the detection of malignant tumors. Negative uptake in malignant tumors seems to be caused by the relatively small size of the tumors. The sensitivity is comparable with a previously reported sensitivity of 69%–89% on conventional CT or MR imaging (*28,29*). Additionally, greater ^{201}Tl activity in viable cancer tissue compared to normal tissue was confirmed in two resected specimens. These findings indicate that ^{201}Tl has a high affinity for malignant tumors in the pancreas and that ^{201}Tl SPECT has potential for positive imaging of pancreatic tumors.

Nearly 50% of the patients in this study required the subtraction technique in order to clarify the boundary be-

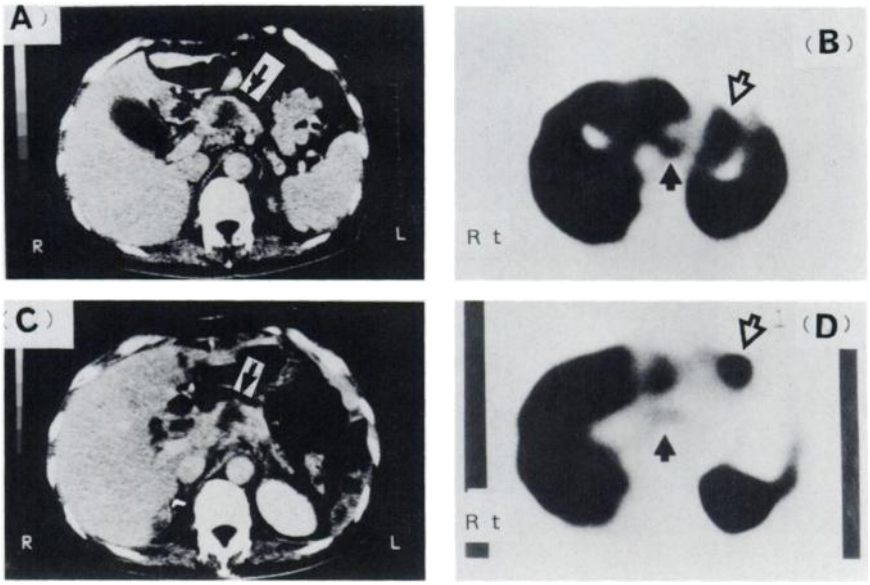

FIGURE 6. A 52-yr-old female with a papillary adenocarcinoma. (A) Pretreatment enhanced CT shows a heterogeneously enhanced 30 × 30 mm tumor in the pancreas head (▶). (B) Pretreatment ^{201}Tl SPECT shows abnormal uptake in the tumor (▶), with an L/H ratio of 0.65. Serum level of CA 19-9 was elevated to 3355 U. Thallium-201 also accumulated in the stomach (▷). The patient underwent intraoperative radiation with a single dose of 20 Gy by electron beam and concomitant hyperthermia at 43°C for 40 min. (C) Enhanced CT performed 14 days after radiation treatment did not show any obvious change in tumor size (▶). (D) The ^{201}Tl SPECT image, however, shows diminished tumor uptake (▶) with an L/H ratio of 0.39. CA 19-9 serum levels also decreased to 564 U. Intense ^{201}Tl uptake in the stomach was seen (▷).

tween abnormal uptake in the pancreatic bed from liver activity (Figs. 4, 5). It is possible that abnormal uptake in these patients might be misinterpreted as a portion of liver activity, which diminishes the sensitivity of the technique. Therefore, we consider that the favorable sensitivity we observed is due to the introduction of this technique. This procedure should be performed when ^{201}Tl SPECT images are uncertain, although it requires a more technically complex process.

In our series, 9 of the 10 patients with chronic pancreatitis showed negative results. One patient with acute pancreatitis and one with focal chronic pancreatitis showed positive ^{201}Tl uptake, but the degree of ^{201}Tl uptake was less intense than that in positive malignant tumors. Complicated pancreatitis in the caudal portion of the tumors is well known (*28*). In our series, however, no clear abnormal accumulation was seen in the caudal portion with secondary dilatation of the pancreatic duct. Togawa et al. (*7*) reported on five of seven patients with chronic pancreatitis that were who had negative images, and Bom et al. (*8*) also reported on five patients with chronic pancreatitis who had negative ^{201}Tl SPECT findings. These results indicate that there is little intense accumulation of ^{201}Tl in pancreatic inflammatory disorders. Previous animal and clinical investigations in other organs or sites have also demonstrated that ^{201}Tl accumulated less intensively in inflammatory lesions than in malignant tumors (*15,30–35*).

Although, our findings showed positive ^{201}Tl uptake in two benign tumors, the degree of uptake is less intense than that in positive malignant tumors. Moreover, previous clinical studies have demonstrated a tendency of less uptake in benign tumors than in malignant tumors (*31–37*). Therefore, the assessment of the degree of ^{201}Tl uptake might be useful in the differentiation of malignant tumors from benign disorders in the pancreas. Further investigation is necessary, however, since we have not yet studied a great number of benign disorders such as pseudotumorous pancreatitis or variable benign neoplasms. Therefore, additional delayed SPECT imaging might also be useful for differential diagnosis. In fact, Bom et al. (*8*) reported several cases of pancreatic cancers in which ^{201}Tl tumor uptake was positive on the delayed image (3 hr postinjection), despite the absence of tumor uptake on the early image.

Frequently, there are many instances of unresectable pancreatic cancers treated conservatively. Therefore, a suitable indicator for monitoring therapeutic outcome is necessary. Tumor markers, especially CA 19-9, have been widely used as one such indicator (*38–43*). Morphologic modalities such as US or CT are routinely used to estimate local tumor response by measuring tumor size. These techniques are of limited value because of the difficulty in adequately differentiating residual viable tumor tissue from necrotic and fibrotic tissues (*44–47*). Thallium-201 may reflect the viability or proliferative potential of the tumor cells (*9–15*), and recent studies have shown that a change in ^{201}Tl uptake in treated tumors can indicate therapeutic response (*17–21*). In the present study, ^{201}Tl uptake in the treated tumors showed alterations similar to those using tumor markers, even in patients with unchanged tumor size.

One disadvantage of using ^{201}Tl SPECT in pancreatic carcinoma is that there might be an interruption of proper visualization of lesional uptake due to small intestinal uptake of ^{201}Tl. Thallium-201 tends to accumulate in the intestine because of active potassium uptake by intestinal mucosa (*7,22,23*), which similarly behaves as ^{201}Tl (*12,14*) moreover, this uptake increases after a meal (*7*). This uptake, however, may be suppressed by fasting (Fig. 1) (*7,22*). In the present study, we employed a lengthy fasting procedure and we did not see more intense intestinal uptake of ^{201}Tl than that in positive malignant tumors.

Our analysis using L/H ratios is problematic for accurate

estimation of the degree of ^{201}Tl uptake because ROIs over the liver will be less affected by an attenuation artifact than those over the pancreatic bed, and the ratio of this attenuation difference may vary from patient to patient. We should emphasize, however, that the L/H ratio acquired with ^{201}Tl SPECT without attenuation correction was used as a semiquantitative index to show the degree of lesional ^{201}Tl uptake. On the other hand, our attempt at attenuation correction resulted in SPECT images with an increased count density of ^{201}Tl in pancreatic lesions with accompanying increased L/H ratios. A simultaneous transmission-emission SPECT system, however, can produce more detailed attenuation maps in each patient and will provide more accurate quantitation of lesional ^{201}Tl uptake (*48,49*).

CONCLUSION

We have evaluated ^{201}Tl SPECT in a group of patients with known pancreatic tumors. Although important morphologic information and high detectability of pancreatic tumors have been offered by other imaging techniques, these modalities do not provide functional information about the tumors, and there are instances in which differential diagnoses could not be clearly confirmed (*44–47,50,51*). Particularly, differentiating between pancreatic cancers and focal pancreatitis on the basis of imaging appearance alone is difficult and may be possible only in typical cases (*28,29*). Similarly, differentiation of complicated pancreatitis from neoplasms may be difficult because of overlapping morphologic features (*29*). Therefore, pancreatic scintigraphy is still important for adequate evaluation of pancreatic diseases, and pancreatic ^{201}Tl SPECT, which has shown good detection capability for malignant tumors and negative or lesser uptake in chronic pancreatitis, is expected to play a role in these issues. Moreover, possible correlation between tumoral ^{201}Tl uptake and tumor markers in patients suggests the use of this modality in monitoring response to treatment.

REFERENCES

1. Antunez AR. Pancreatic scanning with selenium-75-methionine, utilizing morphine to enhance contrast: a preliminary report. *Cleveland Clin Quart* 1964;31:213–218.
2. Yamamoto K, Shibata T, Saji H, et al. Human pancreas scintigraphy using iodine-123-labeled HIPDM and SPECT. *J Nucl Med* 1990;31:1015–1019.
3. Saji H, Kuge Y, Tsutsumi D, Yamamoto K, Konishi J, Yokoyama A. Accumulation and metabolism of ^{125}I-HIPDM in the rat pancreas. *Ann Nucl Med* 1991;5:157–161.
4. Inokuma T, Torizuka T, Magata Y, et al. The usefulness of ^{18}F-FDG-PET in the diagnosis of pancreatic tumors: a comparison with ^{201}Tl SPECT [Abstract]. *Jpn J Nucl Med* 1993;30:977.
5. Togawa T, Suzuki A, Kato K, et al. Relation between ^{201}Tl to ^{67}Ga uptake ratio and histological type in primary lung cancer. *Eur J Cancer Clin Oncol* 1985;21:925–930.
6. Senga O, Miyakawa M, Shirota H, et al. Comparison of ^{201}Tl chloride and Ga-67 citrate scintigraphy in the diagnosis of thyroid tumor: concise communication. *J Nucl Med* 1982;23:225–228.
7. Togawa T, Yui N, Kinoshita F, Koakutsu M, Ryu M, Yamazaki M. Diagnosis of pancreatic cancer using ^{201}Tl-chloride and a three-head rotating gamma camera SPECT system. *Jpn J Nucl Med* 1991;28:1475–1481.
8. Bom HS, Song HC, Kim JY, et al. Usefulness of thallium-201 abdominal SPECT in the evaluation of periampullary tumor [Abstract]. *J Nucl Med* 1994;35:109.
9. Schweil AM, McKillop JH, Miltroy R, et al. Thallium-201 scintigraphy in the staging of lung cancer, breast cancer and lymphoma. *Nucl Med Commun* 1990;11:263–269.
10. Ellingsen JD, Thompson JE, Frey HE, Kruuv J. Correlation of (Na^+-K^+)-ATPase activity with growth of normal and transformed cells. *Exp Cell Res* 1974;87:233–240.
11. Atkins HL, Budinger TF, Leebowitz E, et al. Thallium-201 for medical use. Part III: human distribution and physical imaging properties. *J Nucl Med* 1977;18:133–140.
12. Schweil AM, Mckillop JH, Milroy R, Wilson R, Abdel-Dayem HM, Omar YT. Mechanism of ^{201}Tl uptake in tumours. *Eur J Nucl Med* 1989;15:376–379.
13. Muranaka A. Accumulation of radioisotopes with tumor affinity: comparison of the tumor accumulation of ^{67}Ga-citrate and ^{201}Tl-chloride in vitro. *Acta Med Okayama* 1981;35:85–92.
14. Gehring PJ, Hammand PB. The interrelationship between thallium and potassium in animals. *J Pharmacol Exp Ther* 1976;155:187–201.
15. Ando A, Ando I, Katayama M, et al. Biodistribution of ^{201}Tl in tumor-bearing animals and inflammatory lesion-induced animals. *Eur J Nucl Med* 1987;12:567–572.
16. Black KL, Hawkins RA, Kim KT, Becker DP, Lerner C, Marciano D. Use of thallium-201 SPECT to quantitate malignancy grade of gliomas. *J Neurosurg* 1989;71:342–346.
17. Yoshii Y, Satou M, Yamamoto T, et al. The role of thallium-201 single photon emission tomography in the investigation and characterisation of brain tumors in man and their response to treatment. *Eur J Nucl Med* 1993;20:39–45.
18. Nishigauchi K. Evaluation of feasibility of ^{201}Tl-Cl scintigraphy for monitoring radiotherapeutic effects. *Nippon Acta Radiol* 1993;53:1445–1457.
19. Suga K, Nishigauchi K, Fujita T, Nakanishi T. Experimental evaluation of the usefulness of ^{201}Tl-chloride scintigraphy for monitoring radiotherapeutic effects. *Nucl Med Commun* 1994;15:128–139.
20. Terui S, Terauchi T, Abe H, et al. On clinical usefulness of ^{201}Tl scintigraphy for the management of malignant soft tissue tumors. *Ann Nucl Med* 1994;8:55–64.
21. Ramanna L, Waxman AD, Binney G, et al. Thallium-201 scintigraphy in bone sarcoma: comparison with gallium-67 and technetium-99m-MDP in evaluation of chemotherapy response. *J Nucl Med* 1990;31:567–572.
22. Cavailoles F, Vitaux F, Petiet A, et al. Thallium uptake in fasted and nonfasted rats. *Eur J Nucl Med* 1983;8:87–88.
23. Gupta BL, Hall TA, Naftalin RJ. Microprobe measurement of Na, K and Cl concentration profiles in epithelial cells and inter cellular spaces of rabbit ileum. *Nature* 1978;272:70–73.
24. Yang DC, Bagasa E, Gould L, et al. Radionuclide simultaneous dual-isotope stress myocardial perfusion study using the "three window technique." *Clin Nucl Med* 1993;18:852–857.
25. Budinger TF, Gullberg GT, Huesman RH. Emission computed tomography. In: Herman GT, ed. *Image reconstruction from projections: implementation and application*. New York: Springer-Verlag; 1979:147–246.
26. Moore SC. Attenuation compensation in computed emission tomography. In: Ell PJ, Holman BL, eds. *Emission computed tomography*. New York: Oxford University Press; 1982:339–360.
27. Chang LT. A method for attenuation correction in radionuclide computed tomography. *IEEE Trans Nucl Sci* 1978;25:638–643.
28. Muller MF, Meyenberger C, Bertschinger P, et al. Pancreatic tumors: evaluation with endoscopic US, CT, and MR imaging. *Radiology* 1994;190:745–751.
29. Megibow AJ. Pancreatic adenocarcinoma: designing the examination to evaluate the clinical questions. *Radiology* 1992;183:297–303.
30. Ito Y, Muranaka A, Harada T, et al. Experimental study on tumor affinity of ^{201}Tl-chloride. *Eur J Nucl Med* 1978;3:81–85.
31. Ochi H, Sawa H, Fukuda T, et al. Thallium-201 chloride thyroid scintigraphy to evaluate benign and/or malignant nodules—usefulness of the delayed scan. *Cancer* 1982;50:236–240.
32. Tonami N, Shuke N, Yokoyama K, et al. Thallium-201 single photon emission computed tomography in the evaluation of suspected lung cancer. *J Nucl Med* 1989;30:997–1004.
33. Tonami N, Yokoyama K, Taki J, et al. Thallium-201 SPECT in the detection of mediastinal lymph node metastases from lung cancer. *Nucl Med Commun* 1991;12:779–792.
34. Waxman AD, Ramanna L, Memsic LD, et al. Thallium scintigraphy in the evaluation of mass abnormalities of the breast. *J Nucl Med* 1993;34:18–23.
35. Lee VW, Sax EJ, McAneny DB, et al. A complementary role for thallium-201 scintigraphy with mammography in the diagnosis of breast cancer. *J Nucl Med* 1993;34:2095–2100.

36. Suga K, Sadanaga Y, Nishigauchi K, et al. Lobar primary lymphoma: iodine-123-iodoamphetamine and thallium-201-chloride scintigraphic findings. *J Nucl Med* 1993;34:1980–1983.
37. Suga K, Nishigauchi K, Fujita T, et al. Difference of thallium-201 kinetics between VX-2 tumors and inflammatory lesions in rabbits. *Jpn J Nucl Med* 1994;31:151–161.
38. Tian F, Appert HE, Myles J, Howard JM. Prognostic value of serum CA 19-9 levels in pancreatic adenocarcinoma. *Ann Surg* 1992;215:350–355.
39. Haglund C, Roberts PJ, Kuusela P, Scheinin TM, Makela O, Jalanko H. Evaluation of CA 19-9 as a serum tumour marker in pancreatic cancer. *Br J Cancer* 1986;53:197–202.
40. Satake K, Chung YS, Umeyama K, Takeuchi T, Kim YS. The possibility of diagnosing small pancreatic cancer (less than 4.0 cm) by measuring various serum tumor markers. A retrospective study. *Cancer* 1991;68:149–152.
41. Safi F, Rascher R, Bittner R, et al. High sensitivity and specificity of CA 19-9 for pancreatic carcinoma in comparison to chronic pancreatitis: serological and immunohistochemical findings. *Pancreas* 1987;2:397–401.
42. Glenn J, Steinberg WM, Kurtman SH, et al. Evaluation of the utility of a radioimmunoassay for serum CA 19-9 levels in patients before and after treatment of carcinoma of the pancreas. *J Clin Oncol* 1988;6:462–467.
43. De Villano BC, Brenna S, Brock P, et al. Radioimmunometric assay for a monoclonal antibody-defined tumor marker CA 19-9. *Clin Chem* 1983;29: 549–552.
44. Mackie CR, Cooper MJ, Lewis MH. Nonoperative differentiation between pancreatic cancer and chronic pancreatitis. *Ann Surg* 1979;189:480–487.
45. Jenkins J, Braganza J, Hickey D, et al. Quantitative tissue characterization in pancreatic disease using magnetic resonance imaging. *Br J Radiol* 1989; 60:333–341.
46. Megibow AJ. Pancreatic adenocarcinoma: designing the examination to evaluate the clinical questions. *Radiology* 1992;183:297–303.
47. Semelka RC, Ascher SM. MR imaging of the pancreas. *Radiology* 1993; 188:593–602.
48. Tan P, Bailey DL, Meikel SR, et al. A scanning line source for simultaneous emission and transmission measurements in SPECT. *J Nucl Med* 1993;34: 1752–1760.
49. Wang H, Jaszczak RJ, McCormick JW, et al. Attenuation map determination using Ce-139 with Tc-99m emission radioisotopes in patients [Abstract]. *Eur J Nucl Med* 1994;21:18.
50. Gazelle GS, Mueller PR, Raafat N, et al. Cystic neoplasms of the pancreas: evaluation with endoscopic retrograde pancreatography. *Radiology* 1993; 188:633–636.
51. Bares R, Klever P, Hauptmann S, et al. Fluorine-18-fluorodeoxyglucose PET in vivo evaluation of pancreatic glucose metabolism for detection of pancreatic cancer. *Radiology* 1994;192:79–86.

Scatter

(Continued from page 3A)

to a more strenuous exercise program. His physician ordered a thallium stress test. During treadmill exercise, his EKG remained normal except for the preexisting Q waves and he reached the appropriate pulse rate. A small defect is seen in the anteroapical myocardium consistent with the history of the previous infarction. No ischemic areas are seen. There is no evidence of additional physiologic significant coronary artery disease. APPROVED.

Case 3: A 19-yr-old college freshman had a history of persistent right hip pain. The x-ray of the area was abnormal: probable osteogenic sarcoma in the right ischium. A bone scan is requested to evaluate further the extent of involvement prior to planned chemotherapy and resection of the lesion. He is to undergo amputation of the right leg and hemipelvectomy. The scan is technically excellent, revealing no other areas of involvement. The resident's report is correct and concise. My choices are to "approve, disapprove, edit or skip." How can I simply type "A" for "APPROVE." The scan is correct, but I do not approve of a 19-yr-old man having his leg and hemipelvis amputated. I do not approve of osteogenic sarcoma. Nor do I approve of the pain and suffering in the imaging rooms, the waiting area and elsewhere throughout the center.

After a few more moments of frustration and silent rage, I sigh quietly. I type the letter "A" and call up the next case.

Stanley J. Goldsmith, MD

Editor-in-Chief, The Journal of Nuclear Medicine

May 1995